ISSN 2070-2051, Protection of Metals and Physical Chemistry of Surfaces, 2021, Vol. 57, No. 4, pp. 735–744. © Pleiades Publishing, Ltd., 2021.
Russian Text © The Author(s), 2021, published in Fizikokhimiya Poverkhnosti i Zashchita Materialov, 2021, Vol. 57, No. 4, pp. 407–416.

NANOSCALE AND NANOSTRUCTURED MATERIALS AND COATINGS

Kinetics of Oxidation of Composites Based on Arrays of Multiwalled Carbon Nanotubes and Tin Oxide Obtained by the Magnetron Sputtering Method

S. N. Nesov[a, b], P. M. Korusenko[b, *], V. V. Bolotov[a], K. E. Ivlev[a], S. N. Povoroznyuk[a], and Yu. A. Sten'kin[a]

[a] *Omsk Scientific Research Center, Siberian Branch, Russian Academy of Sciences, Omsk, 644024 Russia*
[b] *Omsk State Technical University, Omsk, 644050 Russia*
**e-mail: korusenko_petr@mail.ru*

Received February 11, 2020; revised May 5, 2020; accepted May 19, 2020

Abstract—The structure, morphology, and chemical state of composites based on arrays of multiwalled carbon nanotubes and tin oxide (SnO_x/MWCNT) obtained using the method of magnetron sputtering were studied using the scanning electron microscopy, transmission electron microscopy, energy-dispersive X-ray spectroscopy, and near edge X-ray absorption fine structure methods. It has been shown that porous layers with a defective structure containing Sn(II) and Sn(IV) oxides along with tin metal were formed on the surface of the MWCNT, which were transformed into crystalline Sn(IV) oxide with a tetragonal lattice at a temperature of ~550°C. The special characteristics of the oxidation and crystallization of the composite components depending on the modes of thermal treatment have been studied. It has been demonstrated that varying the modes of thermal treatment enabled nanostructured materials to be formed that differed significantly in structure, morphology, and composition. It has been hypothesized that the special aspects of the transformation of the composite structure in the process of thermal treatment were determined by the presence of contact of the MWCNT surface with atmosphere.

Keywords: multiwall carbon nanotubes, tin oxide, composites, magnetron sputtering, oxidation, crystallization, electron microscopy, X-ray absorption spectroscopy, synchrotron radiation

DOI: 10.1134/S2070205121040183

1. INTRODUCTION

The formation of composites based on arrays of carbon nanotubes (CNTs) and oxides of different metals is one way to obtaining new materials with a high specific surface area. In particular, composites based on CNTs and tin oxide (SnO_2) are promising in the development of sensitive elements of gas sensors [1, 2] and electrodes of chemical batteries [3, 4]. Effective fixation of preformed metal or metal oxide nanoparticles on CNTs (so-called ex situ methods for formation of composites) is a rather difficult task related to the need to functionalize the chemically inert surface of the latter [5]. The increase of free energy of the surface layers of carbon nanotubes was attained by creating structural defects and attaching different functional groups [5, 6]. For this purpose, CNTs are treated in a medium of different aggressive reagents [5, 6] and exposed to ion-plasma impact [7].

The application of the magnetron sputtering method enables one to form MeO_x/CNT composites, in which metal oxide layers coat the surface of carbon nanotubes sufficiently homogeneously repeating the geometry of the array surface, without the use of prefunctionalization [8]. High adhesion of metal oxide layers to the surface of carbon nanotubes, in this case, is provided due to structural defects formed under the effect of deposited particles and intense impact of atoms and ions of the working gas elastically reflected from the sputtered target. The energy of these particles is in the range of ~10–100 eV, which is higher than the energy of vacancy formation in the graphene plane [9, 10]. However, the layers of metal oxides deposited using the magnetron-sputtering method are often highly heterogeneous in composition and structure [11], which limits the practical application of the composites formed. Most often, thermal treatment in air and oxygen atmosphere are used to optimize the structural and chemical state of metal oxide layers or nanoparticles. For MeO_x/CNT composites, the crystallization temperature of metal oxide could be higher than the temperature of thermal destruction of carbon nanotubes due to their oxidation. Here, the presence of a solid porous layer of metal oxide on the surface of carbon nanotubes enables one to control the structure and composition of the composite in a wide range by

varying the modes of thermal treatment (temperature, heating rate, etc.).

In the present work, changes in the morphology and structure of composites based on multiwall carbon nanotube arrays and tin oxide (SnO_x/MWCNTs) formed using the magnetron sputtering method under thermal treatment conditions at different temperature modes were studied by means of near edge X-ray absorption fine structure (NEXAFS), energy-dispersive X-ray (EDX) spectroscopy, and scanning electron microscopy (SEM) as well as transmission electron microscopy (TEM). The thermal oxidation kinetics of the composites was studied on the basis of the obtained experimental data. It has been demonstrated that varying the modes of thermal treatment enabled us to form nanostructured materials that differed significantly in structure, morphology, and composition.

2. EXPERIMENTAL

To create the composites, arrays of vertically oriented MWCNTs were used that were synthesized on silicon substrates with a surface oxide by the chemical-vapor deposition (CVD) method during pyrolysis of a mixture of acetonitrile and ferrocene (100 : 1). The thickness of the MWCNT layers grown on the substrate was ~15 ± 2 μm. The average outer diameter of a MWCNT was ~40–80 nm. The formation of SnO_x/MWCNT composites by magnetron sputtering was carried out by sputtering a target of metallic tin (99.9% purity) in an argon atmosphere and residual gases at a pressure of 8×10^{-4} Torr. The value of the discharge current was 100 mA at a voltage of 500 V. The duration of deposition of the metal oxide component on the MWCNT surface varied during the formation of composites. Composites formed for 15 min (mode 1) and 30 min (mode 2) of target sputtering were studied, while the other conditions of the magnetron sputtering process were the same.

The thermal treatment of the formed composites was carried out in a tubular quartz furnace at atmospheric pressure. The samples were heated from room temperature to temperatures of 300, 450, 550, and 700°C. The annealing time of the samples after reaching the annealing temperature was 30 min. The heating rate for all temperature modes was ~10°C/min. Samples of the SnO_x/MWCNT composite formed using mode 2 were subjected to thermal treatment.

Analysis of the structure and morphology of the obtained composites was conducted by the SEM method using a JEOL JSM 6610 LV electron microscope at the Omsk Regional Shared Equipment Center SB RAS. The value of the accelerating voltage was 20 kV. This electron microscope was equipped with an INCA-350 Oxford Instruments attachment, which enabled one to conduct the element analysis of samples by the EDX method. The diameter of the probing electron beam in the EDX study was ~1.5 μm, while the depth of the analysis was more than 10 μm. The structure of SnO_x/MWCNT composites was studied by the TEM method using a JEOL JEM 2200 FS microscope at the resource center "VTAN" of Novosibirsk State University (Novosibirsk, Russia).

The study of the atomic and electronic structure of composites by the method of near-edge X-ray absorption fine structure (NEXAFS) was carried out using the equipment of a RGBL-PES experimental station on the BESSY II electron storage ring at the Helmholtz Center for Materials and Energy (Helmholtz-Zentrum Berlin für Materialien und Energie, Berlin, Germany). The spectra were recorded in the mode of measuring the leakage current from the sample with a change in the photon energy of the monochromatic exciting radiation. The resolution of a monochromator was ~0.1 eV. The leakage current was recorded using a Keithley-617 picoammeter. The measurements were carried out in an ultrahigh vacuum atmosphere of $\sim 10^{-9}$ Torr. The size of the exciting synchrotron radiation beam was $\sim 100 \times 100$ μm^2. The depth of the analysis by this method was ~10–20 nm [12]. The measured spectra were normalized to the leakage current measured on a pure gold sample. For the tin absorption spectra (Sn $M_{4,5}$-edge of absorption), the background subtraction procedure was additionally applied.

3. RESULTS AND DISCUSSION

3.1. Analysis of Structure and Chemical State of Initial Composites

Figure 1 shows the SEM images of the initial arrays of the MWCNTs. Analysis of the image data showed that the carbon tubes in the arrays were oriented perpendicularly to the substrate, but, in the upper array layers, there was a significant deviation of individual MWCNTs from the perpendicular orientation. The outer diameter of the MWCNTs was in the range of ~40–80 nm. SEM images of end cleavages (Fig. 1b) showed that the height of the arrays was ~10–12 μm at different areas.

Figure 2 shows SEM images of SnO_x/MWCNT composites formed in modes 1 and 2. One can observe that tin oxide was deposited on the MWCNT array's surface layer sufficiently homogeneously coating the surface of individual carbon nanotubes and tows of them with a continuous layer. Analysis of SEM image of end cleavages of composite (Fig. 2b) showed that the deposition of tin oxide in the form of a continuous layer occurred mainly in the surface layer of the MWCNT array with a thickness of no more than ~3–4 μm. An increase in the synthesis time of the composite resulted in a uniform increase in the metal oxide layer thickness on the surface of carbon nanotubes without the formation of any tin oxide conglomerates in the intertubular space of the MWCNT array. The conducted evaluation showed that the thickness of the

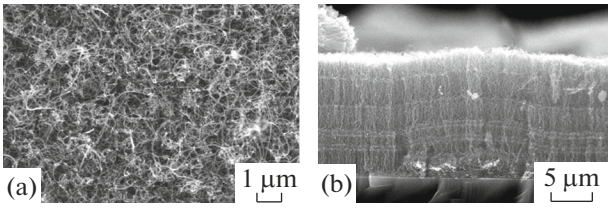

Fig. 1. SEM images of the initial MWCNT array: (a) top view; (b) end cleavage.

tin oxide layer coating the individual MWCNTs in the surface area of the composites was not less than 10 nm for the composite formed in mode 1 and not less than 20 nm for the composite formed in mode 2. The observed structure and morphology and the dynamics of the formation of composites at magnetron sputtering time increase indicated sufficiently high adhesion of the metal oxide layer to the walls of the MWCNTs. Graphite-like materials (graphite, graphene, CNTs), which do not have structural defects, are known to have a sufficiently low wettability in relation to metals and metal oxides [5]. Consequently, high adhesion of tin oxide to the walls of the MWCNTs could result from changes in the structural and chemical states of their surface during the composite formation.

The energy of tin atoms deposited by magnetron sputtering could attain ~30 eV when reaching the substrate. In addition, as was shown in [9, 10], the substrate underwent a significant effect of the working gas atoms and ions elastically reflected from the target during ion sputtering. The energy of these particles was several dozens of electron volts (it could reach ~100 eV), and the fraction of these atoms and ions could reach ~20% of all the atoms of the working gas falling on the target. Thus, the surface of the MWCNTs during the composite formation undergoes an energy effect that can result in the formation of structural defects of the vacancy type (the formation energy of a vacancy in the graphene plane was ~7.5–7.8 eV [13–15]), which, apparently, provides a homogeneous distribution of tin oxide over the surface of carbon nanotubes. Table 1 shows the results of quantitative element analysis of composites according to EDX data.

The atomic concentration of tin in the composites was equal to ~0.3–0.6 at % (Table 1) despite the presence of continuous layers of metal oxide on the MWCNT surface observed in SEM images of composites (Figure 2). This result was caused by high probing depth of the EDX method, which significantly increased the thickness of the composite layers formed on the MWCNT arrays. The presence of silicon in the results of quantitative analysis is related to the signal from the growth substrates. The presence of a small amount of iron is related to the presence of carbon nanotube growth catalyst particles in the cavities and on the surface of the MWCNTs [16]. The rather high oxygen content in the composites indicates that

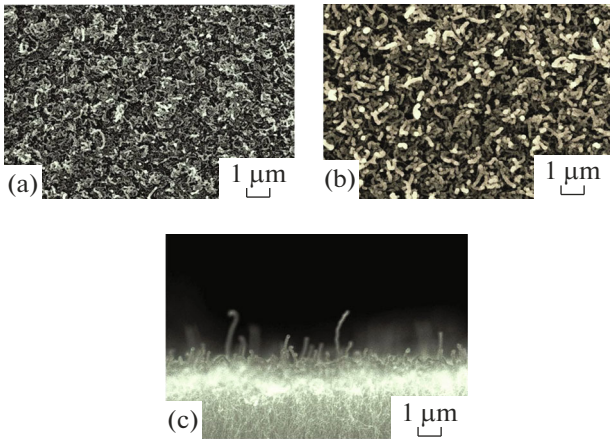

Fig. 2. SEM images of (a) the SnO_x/MWCNT composite (mode 1), (b) the SnO_x/MWCNT composite (mode 2), and (c) the SEM images of the end cleavage of the SnO_x/MWCNT composite (mode 2).

the tin has an oxidized state, as well as possible oxidation of the MWCNT surface during the formation of composites.

Figure 3 shows the TEM image of the SnO_x/MWCNT composite (mode 2). In the image, individual MWCNTs were observed as coated with a uniform layer of tin oxide in sufficiently extended areas. The enlarged image fragment (Fig. 3b) clearly shows that the oxide layer had a porous structure. The observed extended pores spread from the surface of the tin oxide layer to the surface of the carbon nanotube. Thus, the MWCNT surface, even in areas coated with a "continuous" layer of oxide, has a direct contact with the external atmosphere at certain points.

3.2. Effect of Thermal Treatment on Composite Structure

To analyze changes in the structure and morphology, as well as to study the dynamics of oxidation and crystallization of tin oxide and MWCNTs during heat treatment in air, the composites were annealed at temperatures of 300, 450, 550, and 700°C in a quartz tube furnace. The composites were heated from room temperature to one of the specified temperatures, after which they were held in the isothermal mode for 30 min. The selection of annealing temperatures was determined by the limit of the MWCNT stability in air (~350–400°C) [17] and by the temperature characteristic of the initiation of recrystallization processes in tin oxide (450–550°C) [18]. After the thermal treatment, the composites were analyzed by SEM, EDX, and NEXAFS methods. The SnO_x/MWCNT composites formed within 30 min (mode 2) underwent thermal treatment and subsequent analysis.

Figure 4 shows SEM images of SnO_x/MWCNT composites after thermal treatment at temperatures of 450 and 550°C. Note that the structure and morphol-

Table 1. Element composition of SnO_x/MWCNT composites formed under different modes according to EDX data

SnO_x/MWCNT composite (mode 1)					
Point no.	concentration, at %				
	[C]	[O]	[Sn]	[Fe]	[Si]
1	83.4	3.5	0.3	0.3	12.5
2	81.8	3.9	0.3	0.3	13.7
3	81.7	4.1	0.4	0.2	13.6
Average value	82.30	3.83	0.33	0.27	13.27
SnO_x/MWCNT composite (mode 2)					
Point no.	concentration, at %				
	[C]	[O]	[Sn]	[Fe]	[Si]
1	83.0	4.7	0.5	0.2	11.6
2	81.9	6.1	0.5	0.3	11.2
3	80.8	6.6	0.6	0.3	11.7
Average value	81.90	5.80	0.53	0.27	11.50

ogy of the composite after thermal treatment at 300°C virtually did not change; therefore, the corresponding images are not provided in the present work. As can be seen in Fig. 4a, the morphology and structure characteristic of the initial composite were preserved in the composite surface layer after thermal treatment at 450°C. However, the SEM image of the end cleavage indicated that a strong bending of individual MWCNTs was observed in the lower layers of the array, and a noticeable decrease of the array height, which must be a result of oxidation and partial destruction of MWCNT during thermal treatment. This was in good agreement with the results of quantitative EDX analysis (Table 2), which indicated a decrease in carbon concentration and increase in silicon concentration (the signal from the substrate) in the composite after this annealing mode.

As can be seen in Figs. 4c and 4d, the morphology and structure of the composite after annealing at a temperature of 550°C changed significantly. The surface layer of the composite was transformed into a porous layer consisting of globules of a size of ~100 nm with a shape close to spherical. Herewith, the SEM image of the end cleavage indicated that the height of the composite layer significantly decreased after this thermal treatment mode and was about ~3–4 μm (Fig. 4e). Note that the thickness of the porous layer consisting of spherical globules virtually coincided with that of the initial composite layer formed on the surface of the MWCNT array. The formed porous layer had a similar globular structure—both in the surface region and near the silicon substrate (Figs. 4e, 4f, 4g). The presented images indicate the complete destruction of MWCNTs coated with oxide layers in the surface layers of the composite, as well as the destruction of MWCNTs not coated with tin oxide located in the underlying layers of the array. Complete absence of carbon in the results of quantitative EDX analysis (Table 2) confirmed the destruction of carbon nanotubes under this thermal treatment mode. The results shown in Table 2 suggest that the observed globules contained mainly tin oxide with insignificant inclusions of iron or its oxides. A significant decrease of the signal from the substrate in the results of quantitative EDX analysis for the sample after thermal treatment at 550°C related to a density increase of the composite layer due to the destruction of the MWCNTs.

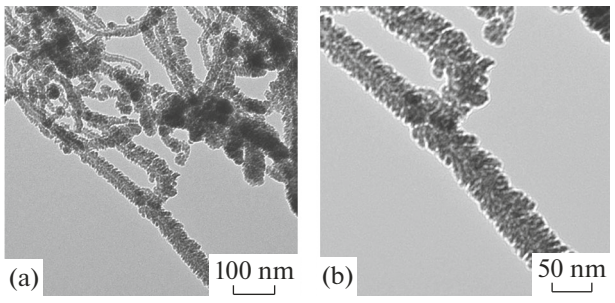

Fig. 3. TEM images of the SnO_x/MWCNT composite (mode 2).

A detailed study of the changes in the atomic structure and chemical state of the carbon and metal oxide components of composites as a result of thermal treatment in air was carried out using near-edge X-ray absorption fine structure (NEXAFS) spectroscopy.

Figure 5 presents the NEXAFS spectra of the SnM-edge of the SnO_x/MWCNT composite after dif-

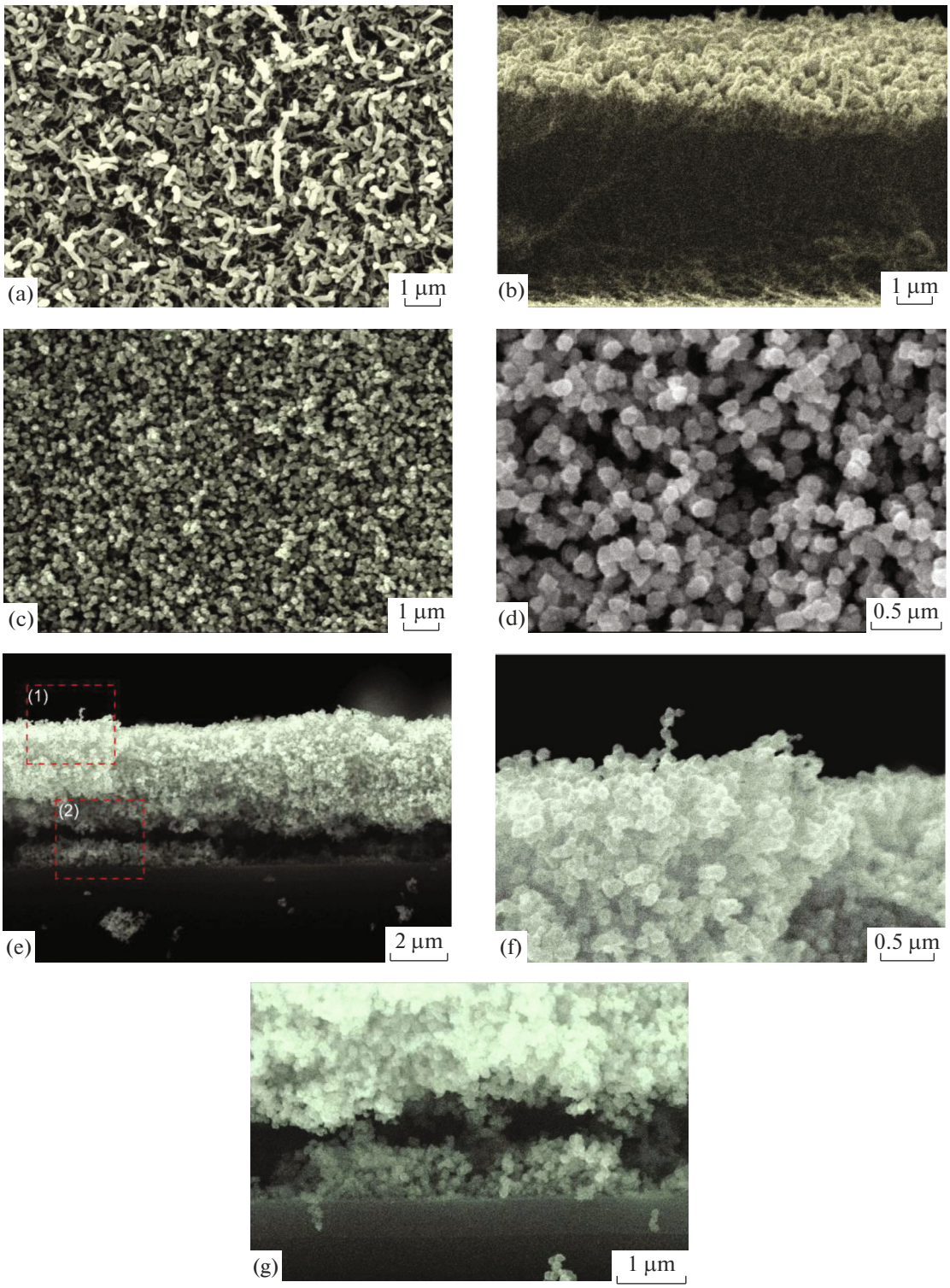

Fig. 4. SEM images of the SnO_x/MWCNT composite (mode 2) (a, b) after annealing in air at 450°C (surface and end cleavage, respectively), (c, d) after annealing in air at 550°C (surface at different magnifications), (e) after annealing in air at 550°C (end cleavage), and (f, g) magnified areas (*1*) and (*2*), respectively.

ferent annealing temperature conditions and the spectrum of the crystalline tetragonal SnO_2 powder, which was used as a reference standard. The NEXAFS Sn M-edge spectrum of the initial SnO_x/MWCNT composite (Fig. 5, curve *1*) did not have the fine structure characteristic of the spectrum of the crystalline tin

Table 2. Element composition of SnO_x/MWCNT composites (mode 2) after thermal treatment at different temperatures according to EDX data

SnO_x/MWCNT composite (mode 2), annealing at 450°C					
Point no.	concentration, at %				
	[C]	[O]	[Sn]	[Fe]	[Si]
1	66.4	6.9	0.4	0.2	26.1
2	65.7	8.4	0.4	0.2	25.3
3	66.5	6.9	0.3	0.2	26.1
Average value	66.20	7.40	0.37	0.20	25.83
SnO_x/MWCNT Composite (mode 2), annealing at 550°C					
Point no.	concentration, at %				
	[C]	[O]	[Sn]	[Fe]	[Si]
1	0	68.2	29.6	0.7	1.5
2	0	67.2	30.4	0.8	1.6
3	0	66.8	31.1	0.7	1.4
Average value	0	67.40	30.36	0.73	1.50

oxide (Fig. 5, curve *5*). The main absorption edges (M_5 edge in the photon energy range of ~490–496 eV and M_4 edge in the photon energy range of ~497–503 eV) were represented by wide, weakly structured bands. This indicates significant distortions in the crystal structure of tin oxide. The presence of the initial composite of a high-intensity preedge maximum at photon energies of ~487 eV in the absorption spectrum indicated the presence of a high number of broken chemical bonds due to the presence of oxygen vacancies [19–21]. The local maximum at photon energies of ~496 eV also indicated an oxygen deficiency in the tin oxide composition. According to [20, 21], the observed form of the spectrum could correspond to a mixture of Sn(II) and Sn(IV) oxides with a tetragonal and orthorhombic lattice and with a predominance of Sn(II) oxides (up to ~65%).

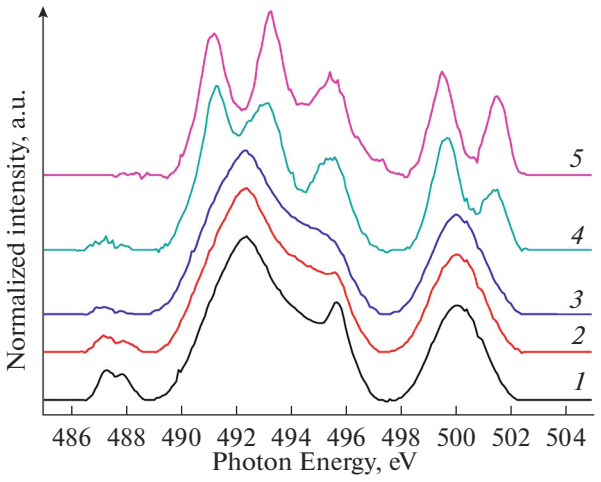

Fig. 5. NEXAFS Sn $M_{5,4}$ spectra (*1*) of the initial SnO_x/MWCNT composite, as well as of the SnO_x/MWCNT composite after thermal treatment at different temperatures: (*2*) 300, (*3*) 450, and (*4*) 550°C; and (*5*) spectrum of the powder of crystalline SnO_2.

Figure 5 shows that the shape of the main edges in the absorption spectra virtually did not change after thermal treatment of the composite at the temperatures of 300 and 450°C, (Fig. 5, curves *2*, *3*). There was only a significant decrease of the intensity of the local maxima at the photon energies of ~487 and ~496 eV corresponding to the oxygen vacancies in the tin oxide composition. The observed dynamics of changes in the absorption spectra of the Sn M-edge indicated that, during thermal treatment of the composite up to and including temperatures of 450°C, the tin oxide was gradually oxidized due to the oxygen diffusion from the surface deep into the tin oxide layer. The shape of the NEXAFS Sn M spectrum of the composite annealed at 450°C (Fig. 5, curve *3*) was in good agreement with the experimentally measured and theoretically calculated X-ray absorption spectra for a film containing a mixture of tetragonal orthorhombic Sn(IV) oxide presented in [20, 21].

The absorption spectrum of the Sn M-edge of the SnO_x/MWCNT composite after thermal treatment at 550°C (Fig. 5, curve *4*) shows the presence of a fine structure characteristic of the spectrum of crystalline SnO_2 with a tetragonal crystal lattice (Fig. 5, curve *5*) [20, 21]. The low intensity of the preedge local maximum at a photon energy of ~487 eV indicated an insignificant content of oxygen vacancies in the tin oxide composition. This result enabled one to conclude that

the spherical globules observed in SEM images of the composite after thermal treatment at 550°C (Figs. 4c, 4d) were crystalline tin dioxide with a tetragonal crystal lattice. Thus, the analysis of the X-ray absorption spectra suggests that the thermally initiated transformation of the metal oxide layer containing a mixture of metallic Sn and its oxides Sn(II) and Sn(IV), which had both tetragonal and orthorhombic crystal lattices, into tetragonal SnO_2 dioxide was realized after the complete oxidation of tin due to the oxygen diffusion from the surface deep into the metal oxide layer.

Figure 6 presents the normalized NEXAFS spectra of the C K-edge of the absorption of the initial MWCNT array and also of SnO_x/MWCNT composites after thermal treatment at different temperatures. In the spectrum of the initial MWCNTs (Fig. 6, curve *1*), two maxima were observed at photon energies of ~285.3 and 291.7 eV, which corresponded to the π*(C=C) and σ*(C=C) states of sp^2-hybridized carbon atoms forming the MWCNT framework [22].

In the spectrum of the initial SnO_x/MWCNT composite (Fig. 6, curve *2*), there was a significant decrease of the intensity of the maximum corresponding to the π*(C=C) states, a decrease in the fine structure of the maximum corresponding to the σ*(C=C) states, and the formation of additional states in the photon energy range of 286–291 eV related to the presence of oxygen-containing functional groups of different types (C–OH, C=O, COOH, C–O–C, etc.) [22–25]. All this indicated that there was an increase of the defectiveness of the crystal structure and the oxidation of carbon in the MWCNT walls during the composite formation under the effect of the deposited tin atoms and the atoms and ions of the working gas reflected back from the target. The formed structural defects and functional groups increased the adhesion of metal oxide to the MWCNT surface, thus providing the formation of continuous layers of tin oxide on their surface [8, 26, 27].

Along with the increase of the thermal treatment temperature in the NEXAFS carbon spectra, there was a gradual decrease of the intensity of the maximum corresponding to the π*(C=C) states and an increase of the intensity of the special characteristics of the absorption spectra corresponding to the states of carbon chemically bound to oxygen (Fig. 6, curves *3*, *4*). This result suggests that oxygen penetrated to the MWCNT surface through a porous layer of tin oxide, which resulted in a gradual oxidation of the walls of carbon nanotubes. As a result of the strong oxidation of carbon, MWCNTs were unstable at the increase of thermal treatment temperature to 550°C, which resulted in their destruction and removal of carbon in the form of gaseous carbon oxides ($CO_x\uparrow$).

The latter was indicated by changes in the carbon absorption spectra (Fig. 6, curve *5*). First, the signal intensity for the sample after this thermal treatment mode significantly decreased, and, in order to compare this spectrum in one graph with other curves in

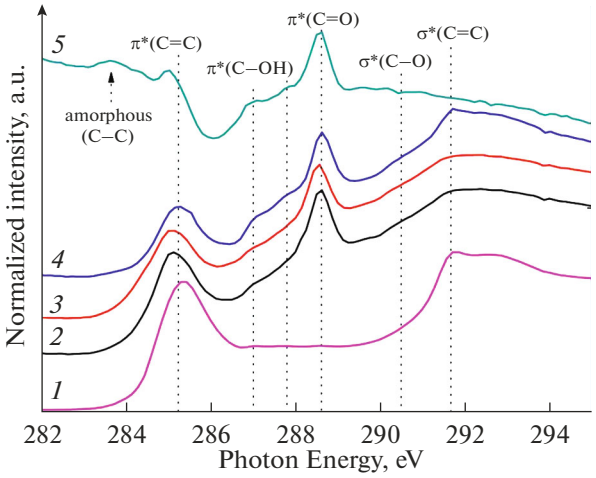

Fig. 6. NEXAFS C–K spectra (*1*) of the initial MWCNT and (*2*) of the initial SnO_x/MWCNT composite (mode 2), as well as of the SnO_x/MWCNT composite (mode 2) after thermal treatment at different temperatures: (*3*) 300, (*4*) 450, and (*5*) 550°C.

Fig. 5, its intensity had to be increased 3 times. The intensity decrease indicated a significant decrease in the carbon amount in the composite. Second, in this spectrum, maxima corresponding to the π*(C=C) and σ*(C=C) states of graphitized carbon were completely absent and there were only intense characteristics corresponding to oxidized forms of carbon, as well as to amorphous carbon. The presence of a weak signal from carbon residues in the absorption spectra of the composite heat-treated at the temperature of 550°C and their complete absence in the data of quantitative EDX analysis (Table 2) resulted from the different sensitivities of these methods to light elements, as well as from a significant difference in the characteristic depth of analysis of these methods.

To further analyze the special characteristics of carbon oxidation and tin oxide crystallization in composites, depending on the heat treatment modes, thermal treatment of the SnO_x/MWCNT composite (mode 2) was conducted at a temperature of 700°C. Figure 7 shows SEM images of the heat-treated composite. Figure 7a shows that the surface after this heat treatment mode preserved the structure and morphology characteristic of the initial composite. A network of individual tubular structures was observed: they must be were carbon nanotubes coated with a tin oxide layer. This result was rather unexpected, since the temperature of the thermal treatment was significantly higher than the limit of the thermal stability of the MWCNTs in air. Analysis of the SEM image of the heat treated composite's end cleavage (Fig. 7b) indicated the thermal destruction of the MWCNTs located in the underlying layers of the array and not coated with a continuous layer of tin oxide, which was a rather expected result. Herewith, according to the

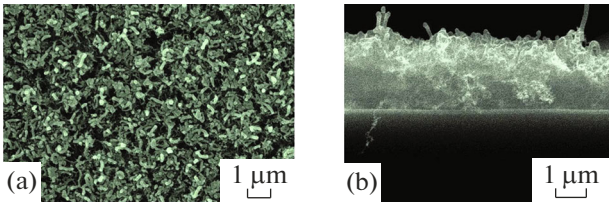

Fig. 7. SEM images of the SnO_x/MWCNT composite (mode 2) after thermal treatment at 700°C: (a) surface; (b) end cleavage.

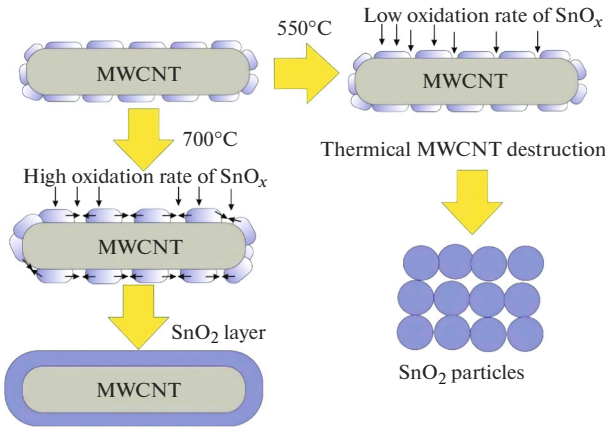

Fig. 8. Schematic model of the transformation of the SnO_x/MWCNT composite structure under thermal treatment conditions at temperatures of 550 and 700°C.

results of the quantitative EDX analysis (Table 3), rather high carbon content (~11–13 at %) was observed in the heat-treated composite. This was evidence in favor of the partial preservation of the MWCNT carbon framework in areas coated with a continuous layer of tin oxide. At comparing the results of quantitative EDX analysis of composite samples heat-treated at temperatures of 550 and 700°C (Tables 2, 3, respectively), the fact of significant differences in concentrations of silicon (the signal from the substrate) and tin in the composition of these samples was notable. A more significant signal from the substrate in the case of a composite heat-treated at a temperature of 700°C must be caused by the lower density of the composite material related to the preservation of the carbon nanotube framework under the tin oxide layer. The low value of the Sn concentration in the sample after thermal treatment at 700°C (Table 3) must be also a consequence of the fact that tin was mainly distributed in the form of thin layers on the surface of the carbon framework.

The observed results indicated changes in the special characteristics of oxidation and crystallization of the composite components at a temperature increase to 700°C. The differences of the processes of oxidation and crystallization in composites under the conditions of thermal treatment at temperatures of 550 and 700°C are shown schematically in Fig. 8.

Apparently, the main factor determining the structure change of the composite at these temperatures was the rate of oxidation and subsequent crystallization of the porous layer of the metal oxide component, which initially had a high oxygen deficiency. Obviously, an increase in the volume during oxidation leads to gradual clogging of the pores existing in the oxide layer of the initial composite, which hinders the access of oxygen to the MWCNT surface. Thermal treatment of the composite at 700°C ensures fast clogging of pores in the tin oxide layer, which prevents oxygen migration to the MWCNT surface and prevents their oxidation. As a result, tin oxide crystallizes in the form of a thin layer on the surface of individual MWCNTs, repeating the geometry of their surface. At a temperature of 550°C, the oxidation process of tin oxide proceeds more slowly, which ensures the contact of carbon nanotubes with the atmosphere at an elevated temperature. This leads to oxidation and thermal destruction of MWCNTs.

CONCLUSIONS

By means of the methods of SEM, TEM, EDX, and NEXAFS, the morphology, structure, and chemical composition of SnO_x/MWCNT composites formed by the magnetron sputtering method and special characteristics of the oxidation and crystallization of the composite components under conditions of thermal treatments in air at different temperatures have been studied. It has been shown that the formation of structural defects and the oxidation of the outer

Table 3. Element composition of SnO_x/MWCNT composites (mode 2) after thermal treatment at a temperature of 700°C according to EDX data

Point no.	Concentration, at %				
	[C]	[O]	[Sn]	[Fe]	[Si]
1	12.3	27.7	1.6	1.2	57.2
2	13.3	24.0	1.3	0.9	60.5
3	11.4	25.3	1.4	1.1	60.8
Average value	12.33	25.67	1.43	1.07	59.50

walls of the MWCNTs proceeded during the process of deposition of tin on the MWCNT surface by the method of magnetron sputtering. This, in its turn, increased the interfacial adhesion in composites and provided the formation of continuous porous layers of the metal oxide component on the surface of individual MWCNTs. It has been established that the layer of the metal oxide component in the initial composites had a highly defective structure and was represented by a mixture of Sn(II) and Sn(IV) oxides with the possible inclusion of metallic Sn. It has been shown that the transformation of a mixture of tin oxides into a crystalline Sn(IV) oxide with a tetragonal crystal lattice proceeded in the temperature range 450–550°C. This was preceded by a gradual oxidation of tin in the temperature range of 300–450°C.

It has been experimentally established that, under thermal treatment conditions at a temperature of 550°C, the process of oxidation and crystallization of tin oxide proceeded slowly and the migration of oxygen through the porous metal oxide layer to the MWCNT surface resulted in oxidation and complete thermal destruction of the latter with the removal of carbon from the composite in the form of gaseous oxides ($CO_x\uparrow$). As a result, a layer of crystalline tin dioxide with a tetragonal crystalline lattice was formed that consisted of dense spherical globules with a diameter of ~100 nm.

When using higher thermal treatment temperatures (700°C), the process of saturation of defective tin oxide with oxygen and subsequent crystallization occurred more quickly, which resulted in blocking of the channels for oxygen diffusion to the MWCNT surface through the tin oxide layer due to a volume increase. As a result, the framework of carbon nanotubes in the areas coated with a continuous metal-oxide layer was preserved and tin oxide crystallized on the surface of individual MWCNTs in the form of thin layers (of a thickness of ~20 nm).

The new nanostructured materials formed as a result of thermal treatments of the initial SnO_x/MWCNT composites may be promising for the development of electrodes for sodium- and lithium-ion batteries, supercapacitors, and sensitive elements of gas sensors. Layers of porous globular crystalline tin oxide (SnO_2) obtained by annealing at 550°C, due to their high surface area, can have increased values of specific capacity along with high sensitivity to different gases. The structure of the material formed by thermal treatment of the initial composite at a temperature of 700°C—in addition to possible high capacitance characteristics—enabled it to be hypothesized that this material has a greater resistance to cyclic volume changes during intercalation/deintercalation of alkali metal ions into tin oxide during battery operation, since the carbon framework located under the crystal tin layer is capable of minimizing the emerging mechanical stresses.

ACKNOWLEDGMENTS

The authors are grateful to the staff of the Omsk Scientific Center of the Siberian Branch of the Russian Academy of Sciences: V.E. Roslikov for the creation of composites by the method of magnetron sputtering. The authors are also grateful to the management of the Omsk Regional Shared Equipment Center SB RAS for providing equipment for the analysis of samples by SEM and EDX methods and to the administration of the Russian–German channel of the BESSY II electron storage ring as well as D.A. Smirnov (beamline scientist at the RGL-PES station) for assistance in conducting studies by the NEXAFS method.

FUNDING

This work was carried out within the governmental order for Omsk Scientific Center of the Siberian Branch of the Russian Academy of Sciences (project registration number 121021600004-7).

REFERENCES

1. Liu, H., Zhang, W., Yu, H., et al., *ACS Appl. Mater. Interfaces,* 2016, vol. 8, p. 840.
2. Majumdar, S., Nag, P., and Devi, P., *Mater. Chem. Phys.,* 2014, vol. 147, p. 79.
3. Alaf, M. and Akbulut, H., *J. Power Sources,* 2014, vol. 247, p. 692.
4. Korusenko, P.M., Nesov, S.N., and Bolotov, V.V., *J. Alloys Compd.,* 2019, vol. 793, p. 723.
5. Rahmandoust, M. and Ayatollahi, M.R., *Adv. Struct. Mater.,* 2016, vol. 39, p. 1.
6. Long, H., Guo, C., Wei, G., et al., *Vacuum,* 2019, vol. 166, p. 147.
7. Acauan, L., Dias, A.C., Pereira, M.B., et al., *ACS Appl. Mater. Interfaces,* 2016, vol. 8, p. 16444.
8. Nesov, S.N., Korusenko, P.M., Bolotov, V.V., et al., *Kondens. Sredy Mezhfaznye Granitsy,* 2018, vol. 20, p. 237.
9. Alexeeva, O.K. and Fateev, V.N., *Int. J. Hydrogen Energy,* 2016, vol. 41, p. 3373.
10. Kuz'michev, A.I., *Magnetronnye raspylitel'nye sistemy* (Magnetron Sputtering Systems), Kyiv: Avers, 2008.
11. Berlin, E.B. and Seidman, L.A., *Poluchenie tonkikh plenok reaktivnym magnetronnym raspyleniem* (Thin Films Synthesizing by means of Reactive Magnetron Sputtering), Moscow: Tekhnosfera, 2014, p. 256.
12. Isomura, N., Murai, T., Nomoto, T., et al., *J. Synchrotron Radiat.,* 2017, vol. 24, p. 1.
13. Yang, G., Kim, B., Kim, K., et al., *RSC Adv.,* 2015, vol. 5, p. 31861.
14. Li, L., Reich, S., and Robertson, J., *Phys. Rev. B,* 2005, vol. 72, article ID 184109.
15. Latham, C.D., Heggie, M.I., Alatalo, M., et al., *J. Phys.: Condens. Matter,* 2013, vol. 25, article ID 135403.
16. Korusenko, P.M., Nesov, S.N., Bolotov, V.V., et al., *Phys. Solid State,* 2017, vol. 59, p. 2045.
17. Mahajan, A., Kingon, A., Kukovecz, A., et al., *Mater. Lett.,* 2013, vol. 90, p. 165.

18. Nesov, S.N., Korusenko, P.M., Bolotov, V.V., et al., *Tech. Phys. Lett.,* 2017, vol. 43, p. 961.
19. Sharma, A., Varshneya, M., Shin., H.J., et al., *Curr. Appl. Phys.,* 2016, vol. 16, p. 1342.
20. Manyakin, M.D., Kurganskii, S.I., Dubrovskii, O.I., et al., *Mater. Sci. Semicond. Process.,* 2019, vol. 99, p. 28.
21. Manyakin, M.D., Kurganskii, S.I., Dubrovskii, O.I., et al., *Comput. Mater. Sci.,* 2016, vol. 121, p. 119.
22. Fedoseeva, Yu.V., Bulusheva, L.G., Koroteev, V.O., et al., *Appl. Surf. Sci.,* 2020, vol. 504, article ID 144357.
23. Fedoseeva, Yu.V., Okotrub, A.V., Bulusheva, L.G., et al., *Diamond Relat. Mater.,* 2016, vol. 70, p. 46.
24. Kuznetsova, A., Popova, I., Yates, J.T., et al., *J. Am. Chem. Soc.,* 2001, vol. 123, p. 10699.
25. Wang, L., Han, J., Zhu, Y., et al., *J. Phys. Chem. C,* 2015, vol. 119, p. 26327.
26. Nesov, S.N., Korusenko, P.M., Povoroznyuk, S.N., et al., *Nucl. Instrum. Methods Phys. Res., Sect. B,* 2017, vol. 410, p. 222.
27. Sivkov, V.N., Ob"edkov, A.M., Petrova, O.V., et al., *Phys. Solid State,* 2020, vol. 62, no. 1, p. 214.

Translated by D. Marinin